Two Base Pair Duplexes Suffice to Build a Novel Material

Martin Meng,[a] Carolin Ahlborn,[a] Matthias Bauer,[a] Oliver Plietzsch,[a] Shahid A. Soomro,[a] Arunoday Singh,[a, b] Thierry Muller,[a] Wolfgang Wenzel,[c] Stefan Bräse,[a] and Clemens Richert*[a, b]

Nature evolved DNA to store genetic information. New applications, including those in the field of nanostructuring, are emerging rapidly for this biomacromolecule. For example, DNA can be used to build artificial shapes,[1] polyhedra[2] and functional nanodevices.[3,4] Further, DNA-coated nanoparticles[5] can be used as diagnostic devices with extreme sensitivity.[6] The structural roles of DNA in setting up nanoscale assemblies[7] and lattices are being discussed.[8,9] This confirms that rule-based DNA duplex formation occurs in non-natural chemical contexts. Less clear, though, is how embedding DNA duplexes in nanostructured environments affects thermodynamic stability, kinetics of hybridization, and cooperativity of formation.

Short DNA duplexes are known to melt cooperatively into single strands. The dissociation process, commonly monitored with UV-melting curves, can be described with a two-state model.[10] Most building blocks of DNA-mediated nanoassemblies bind through more than one strand. Multivalent binding should lead to an increase in binding constant.[11] For three-dimensional nanostructures built from DNA-coated nanoparticles, a surprisingly small change in the melting point over that of linear duplexes is observed, however.[12,13] The same is true for micrometer-scale crystallites formed from DNA-coated spheres.[14] Further, the bigger the assemblies become, the more difficult it should become to achieve cooperative transitions because molecular information has to be transferred over larger and larger distances. Again, this is not what one finds for DNA-coated nanoparticles and polymer-based DNA-dendrimers,[15] which have melting transitions that are exceptionally sharp and thus highly cooperative. Either phenomenon can be explained by a model that takes the electrostatic situation of closely packed DNA strands and the cloud of the surrounding counter ions into account.[12]

While nanoscale objects made of DNA are well established, the generation of quasi-infinite crystalline structures through DNA duplex formation has remained a challenge, probably as a consequence of the complex energetics and cooperativities of duplex formation during the assembly process. Crystallites have been detected in assemblies of DNA-coated gold nanoparticles,[16,17] but single crystals with unit cells held together by base pairing are rare.[18] Porous nanoscale crystals that host catalysts in their cavities or aid structure elucidation for proteins remain difficult targets.[3d]

Here we present DNA hybrids designed to assemble into new materials through more than one DNA chain. These behave differently from DNA-coated nanoparticles and polymer-DNA. Their hybridization properties are also different from three-arm DNA hybrids with a large planar core.[19] The melting point of our hybrids is much higher than that of linear control duplexes, and the transitions are not highly cooperative. Further, the smaller the designed lattice constant, the greater the effect of salt on the stability of the assemblies. A hybrid with two base pairs per duplex forms a new material that precipitates from aqueous solution as a solid at micromolar concentration. In the current study, no attempts were made to crystallize the hybrids, and it would be inappropriate to assume that single crystals, suitable for X-ray diffractometry, will form under melting curve conditions.

We chose hybrids with DNA strands that are preoriented by an organic core (Figures 1 and 2). This design places four DNA strands at the corners of a tetrahedron. While the core is necessarily tetrahedral, due to steric conflicts, a certain flexibility exists for the DNA chains, particularly in single-stranded form. The core also avoids a blurring of melting curve data caused by simultaneous melting of a geometry-defining DNA branch-

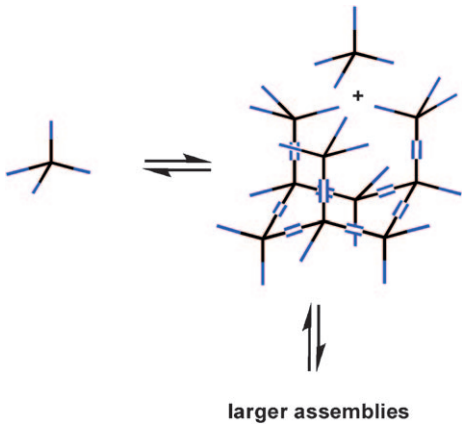

Figure 1. Proposed self assembly of tetrahedral hybrids consisting of an organic core (black) and four DNA strands (blue) into a diamond like lattice. During the assembly process up to three DNA duplexes are formed simultaneously.

[a] *M. Meng, Dr. C. Ahlborn, Dr. M. Bauer, O. Plietzsch, Dr. S. A. Soomro, A. Singh, Dr. T. Muller, Prof. S. Bräse, Prof. C. Richert*
Institut für Organische Chemie and Center for functional Nanostructures (CFN), Universität Karlsruhe (TH)
76131 Karlsruhe (Germany)
Fax: (+49) 721 608 4825
E mail: cr@rrg.uka.de

[b] *A. Singh, Prof. C. Richert*
Current address:
Institut für Organische Chemie, Universität Stuttgart
70569 Stuttgart (Germany)

[c] *Dr. W. Wenzel*
Institute for Nanotechnology, Research Center Karlsruhe
76344 Eggenstein Leopoldshafen (Germany)

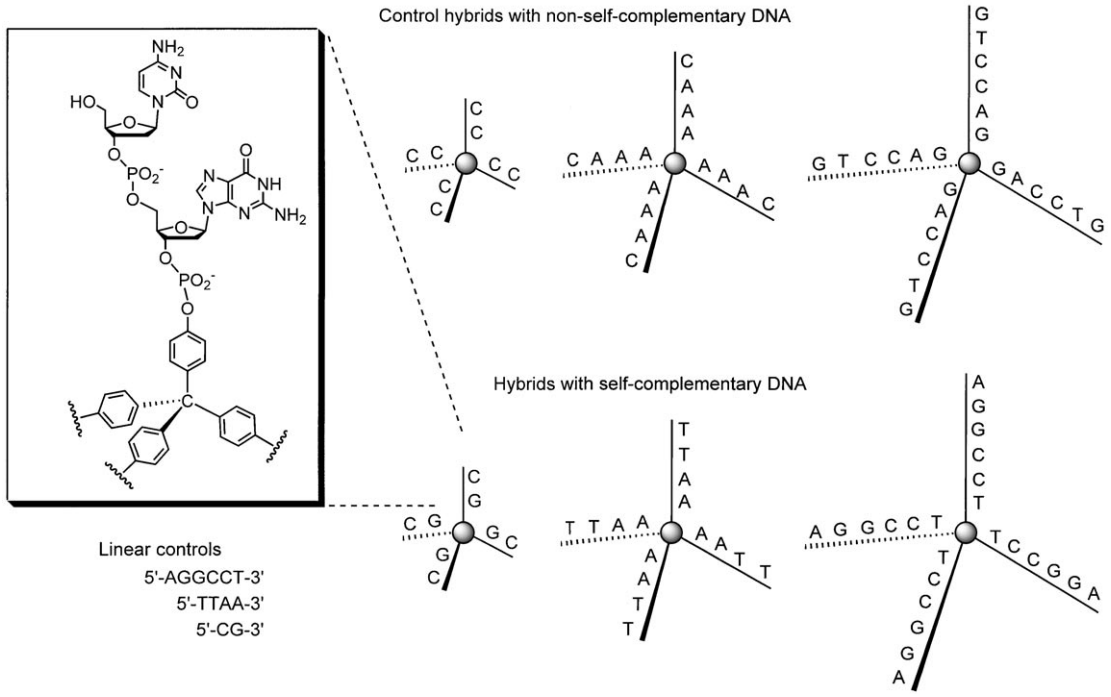

Figure 2. Compounds employed in this study.

ing element and the duplexes of the sticky ends. Our hybrids consist of a tetrakis(*p*-hydroxyphenyl)methane (TPM) core and four DNA strands. Molecular modeling suggests that their structure is suitable for forming four duplexes without steric conflicts (Figure 3). Modeling gives core-to-core distances in the low nanometer range. For example, for the assembly of $(TTAA)_4$TPM the distance is 2.5 nm. We sampled short DNA sequence lengths, assuming that highly cooperative binding events would take place. One possible event that forms three duplexes simultaneously is shown in Figure 1. We note that DNA hybrids with organic cores have been studied before,[3b–d] for example, in the context of two-dimensional assemblies[20] and replication,[21] and so have hybrids with inorganic[22] and dendrimer[23] cores. These studies have focused on hybrids with longer DNA strands and did not lead to a new solid material at micromolar hybrid concentrations in aqueous buffer.

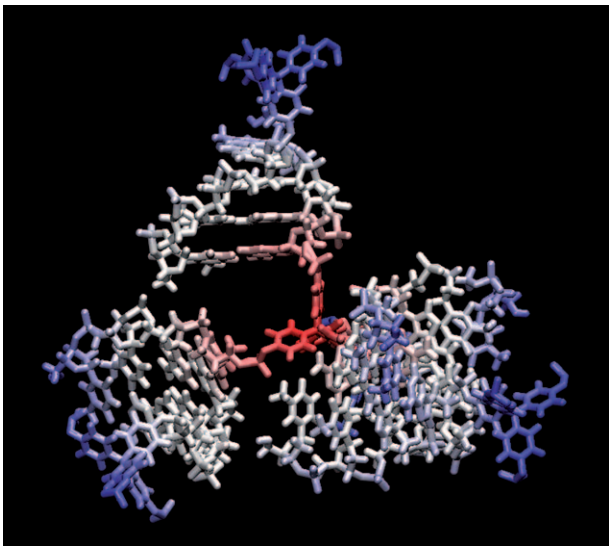

Figure 3. Structure of a core molecule of $(TTAA)_4$TPM surrounded by four DNA duplexes, as obtained by molecular modeling, highlighting the absence of steric conflicts after hybridization to four complementary hybrids. Core region: red; duplex regions: white, and the peripheral region including trun cated cores: blue.

A general synthetic scheme was developed to prepare the tetrahedral DNA hybrids. It involves on-support phosphitylation, microwave-assisted coupling of the unprotected core, and a combination of 3′- and 5′-phosphoramidites that is similar to earlier routes to branched structures.[22, 23, 24] Control hybrids with non-self-complementary DNA sequences were also prepared, together with linear DNA controls (Figure 2). All compounds were characterized mass spectrometrically, and were purified chromatographically to homogeneity. For some hybrids, this required ion-exchange HPLC under denaturing conditions to suppress assembly processes during separation.

Figure 4 shows a typical melting profile for a DNA hexamer motif, both by itself (linear control duplex), and in the context of a hybrid. Three features are striking. First, the melting point is more than 40 °C higher for the hybrid than for the linear duplex (Table 1). Secondly, the sharpness of its melting does not increase for the hybrid. The transition breadth determined from first derivatives is 25 °C for the hybrid and 17 °C for the linear control. Thirdly, a noticeable hysteresis between heating and cooling curve is observed for the tetrahedral structure under the experimental conditions (1 °C heating/cooling per minute); this is a feature atypical for short duplexes. Thus, the assembly takes longer to form than the linear DNA duplex upon cooling, and it is slower to break up upon heating. This

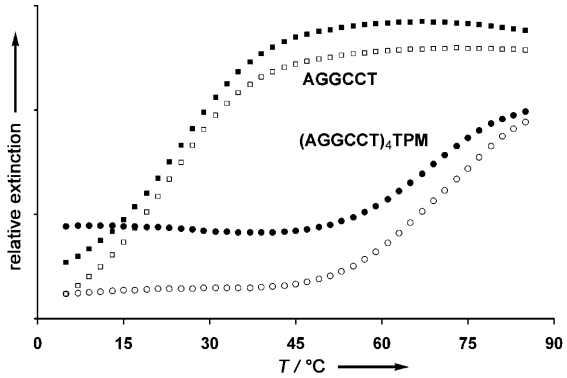

Figure 4. UV melting (heating curves: open symbols, cooling curves: filled symbols) of a hybrid with four self complementary hexanucleotide DNA arms (4 μM) and the corresponding linear control (16 μM) in 10 mM TEAA buffer, 150 mM NaCl, pH 7. Raw data of melting curves can be found in the Supporting Information.

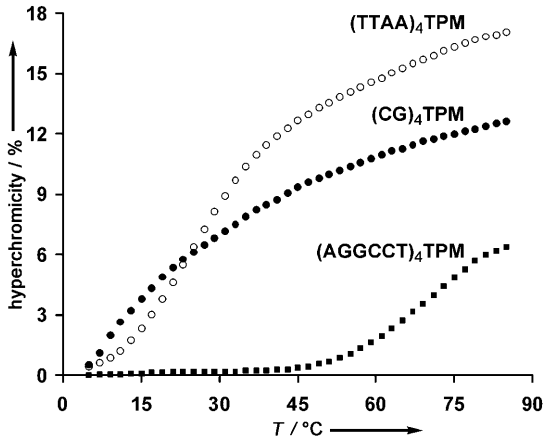

Figure 5. UV melting of hybrids (4 μM) with decreasing DNA chain length in 10 mM TEAA buffer, pH 7.

Table 1. UV melting points [°C] of duplexes or assemblies formed by DNA hybrids and their non self complementary controls at 4 μM hybrid concentration or 16 μM strand concentration for linear controls.

Compound	Buffer[a]	+NaCl[b]	+$MgCl_2$[c]
AGGCCT	18	24	27
$(AGGCCT)_4$TPM	62	70	70
$(GTCCAG)_4$TPM	n.t.[d]	n.t.	n.t.
TTAA	n.t.	n.t.	<15
$(TTAA)_4$TPM	19	26	40
$(CAAA)_4$TPM	n.t.	n.t.	n.t.

[a] 10 mM TEAA buffer, [b] +150 mM NaCl, [c] +100 mM $MgCl_2$, [d] No co operative transition.

suggests the formation of larger structures. There is also a reduced hyperchromicity for the hybrid, as expected for incomplete duplex formation at the fringes of nanoscale assemblies. A control hybrid with a more flexible and a less symmetrical aliphatic core molecule also showed high temperature melting with hysteresis (see Figure S5 in the Supporting Information). This suggests that the effects observed are not limited to hybrids with a TPM core.

The stability of the assemblies of hybrids scales with the stability of the underlying duplexes. Figure 5 shows an overlay of melting curves for hybrids forming hexamer, tetramer and dimer duplexes. The melting point decreases with duplex length, and the effect is modulated by base composition. Weak base pairs between adenine and thymine are less stabilizing than the strong base pairs between cytosine and guanine, so that the melting point of the hybrid with dimer arms is only slightly lower than that of the hybrid with tetramer arms. The melting points observed for the hybrids are not far from those expected for linear duplexes formed by continuous strands that are *four times* the length of one "arm" of the hybrids (for example, 45 °C calculated for TTAATTAATTAATTAA, compared to 40 °C for $(TTAA)_4$TPM at 4 μM concentration; Table S1). For the tetramer or dimer sequence alone, the linear controls do not show melting above 10 °C (Tables 1 and 2). Rapid off-rates and strong background absorbance complicate experiments with a sufficient excess of linear competitor DNA over the strongly assembling hybrids (compare Figure S14 and S15). But, the control hybrids with a non-self-complementary DNA sequence do not give cooperative melting transitions (Figure 6); this confirms that the assembly process is sequence-specific and is not a simple consequence of some structural feature of our hybrids.

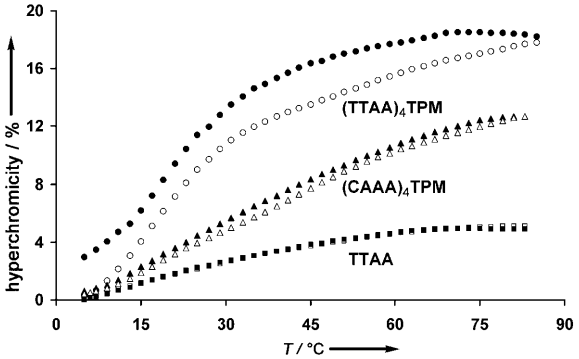

Figure 6. UV melting of a hybrid (heating curves: open symbols, cooling curves: black symbols) with four self complementary nucleotide DNA chains (4 μM), as well as that of a control hybrid with non self complementary DNA (4 μM) and a linear control (16 μM) in 10 mM TEAA buffer, pH 7.

Addition of salts of monovalent (Na^+) or divalent (Mg^{2+}) cations to the buffered solution led to another unexpected effect. The shorter the DNA, and thus the smaller the dimensions of the assembly, the stronger the effect of salt on the melting point (Table 2). Whereas the hexamer-displaying hybrid gives a melting point largely unaffected by the addition of NaCl and $MgCl_2$, the tetramer hybrid gives a strong melting point increase in the presence of the salts. Comparison of the data at 4 μM (Table 1) and 15 μM hybrid concentration (Table 2) shows a measurable increase in melting points in all but two cases, as expected for an intermolecular assembly process and a modest increase in concentration. Again, the effect is stronger

Table 2. UV melting points [°C] of assemblies formed by DNA hybrids at 15 μM concentration.

Compound	Buffer[a]	$+Na^{+}$ [b]	$+Mg^{2+}$ [c]
$(AGGCCT)_4$TPM	61	70	70
$(GTCCAG)_4$TPM	n.t.[d]	n.t.	n.t.
$(TTAA)_4$TPM	20	29	42
$(CAAA)_4$TPM	n.t.	n.t.	n.t.
$(CG)_4$TPM	n.t.	<15	solid[e]
$(CC)_4$TPM	n.t.	n.t.	n.t.

[a] 10 mM TEAA buffer, [b] +150 mM NaCl, [c] +100 mM $MgCl_2$, [d] No co operative transition. [e] precipitation at $\leq$ 15 °C.

for $(TTAA)_4$TPM than for $(AGGCCT)_4$TPM. The unusually strong enhancement of affinity of the DNA chains for each other in the case of the dimer hybrid $(CG)_4$TPM culminates in the formation of a solid precipitate from the aqueous solution. At or below room temperature this compound showed discontinuous melting profiles, caused by scattering on particles forming in the cuvette (see Figure 7). UV absorbance and MALDI measurements as well as control experiments demonstrate that the solid formed is indeed composed of the hybrid and not just an inorganic salt. A strong concentration dependence of this phenomenon was observed for the smallest hybrid. At 4 μM, no precipitate forms, at 15 μM the onset of precipitation is approximately 15 °C, and at 120 μM, precipitation starts at approximately 20 °C.

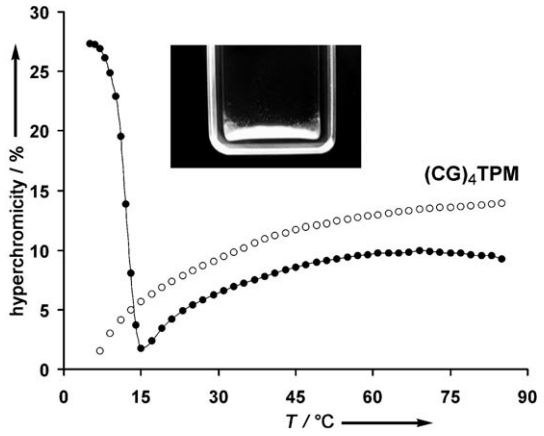

Figure 7. UV monitored assembly process of $(CG)_4$TPM hybrids (15 μM) with just two nucleotides per DNA chain in 10 mM TEAA buffer, pH 7, 150 mM NaCl. ○: Absorbance at 260 nm prior to, and ●: after addition of 100 mM $MgCl_2$, resulting in precipitation upon cooling at 1 °C min $^{-1}$. The increase in apparent hyperchromicity at low temperature is caused by scattering during the initial phase of precipitation. Inset: The photograph shows the cuvette after settling of the precipitate at 4 °C.

According to the available data from solutions ranging from 4–15 μM (hexamer and tetramer hybrid) and 4–150 μM (dimer hybrid), no signs of sharpening of the transition[19] are seen when lowering the concentration. Further, the temperature of the onset of precipitation increases both with increasing salt concentration and with increasing hybrid concentration for $(CG)_4$TPM, again showing no signs of caged dimer formation.

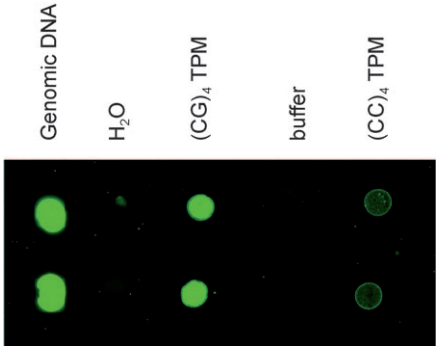

Figure 8. Fluorescence image of samples stained with duplex specific fluo rescent dye YoYo 1. Samples of $(CG)_4$TPM in the presence of 100 mM $MgCl_2$, together with positive (genomic DNA) and negative controls, including non self complementary $(CC)_4$TPM. All samples were spotted in duplicate. See the Supporting Information for details and numerical fluorescence values.

Staining with a duplex-specific dye confirms that base pairing does occur in the assemblies formed by $(CG)_4$TPM (Figure 8).

Our results are significant for the field of DNA-mediated nanostructuring and crystallization on the nanoscale. Earlier work on electrostatically tuned inorganic nanoparticles has shown that successful crystallization requires tempering the strong and cooperatively occurring forces between these particles by using organic coatings that reduce the attraction to van der Waals and weak electrostatic interactions, and thus allow for reversibility and the formation of near perfect crystallites.[25] Similarly, our results show that a CG dinucleotide per DNA arm is sufficient to drive the assembly process and lead to a new material. Hybrids with longer DNA strands give higher melting points than their linear counterparts, statistically coated nanoparticles, or three-arm hybrids.[19] We expect the effect of multivalent binding to be even more pronounced for octahedral cores inducing the formation of six duplexes per hybrid.

In our assemblies, multiple duplex-forming events apparently result in massive increases in binding strength, but the cooperativity of the transition does not increase. So, the electrostatic situation must be different from that of nanoparticle-based assemblies involving long DNA duplexes in close proximity.[12] Perhaps, once the duplexes are short enough and separated by rigid organic cores, there is no longer a counter ion cloud that acts cooperatively. The TPM core probably also prevents a near parallel position of the duplexes. Still, we observe that the assemblies of the shorter DNA strands show a stronger salt dependence than longer strands; this indicates that close packing of the negatively charged backbones does occur.

Our results may also help to explain why earlier studies on oligonucleotide hybrids with inorganic cores and DNA chains of much greater length have led to assemblies without crystalline structure.[22] The future design and experimental realization of DNA-based three-dimensional nanostructures, including designed crystals with nanoscale unit cell dimensions, should take these findings into account. Such crystals have long been regarded as a goal of DNA-based nanostructuring.[3] If two base pairs per duplex are sufficient for assembly, even for

simple tetrahedral designs, minimal sticky ends may be used. This conclusion is corroborated by very recent findings involving very large nanoparticles.[26] Very short duplexes may also mean smaller activation energies for breaking down imperfect structures in dynamic assembly/disassembly processes and would lead to the thermodynamically most stable, perfect crystal lattices more readily. The broad transitions upon cooling observed in our study are encouraging for those who wish to generate crystals based on duplex formation. Automated DNA synthesis and the progress in the synthesis of hybrids may thus lead to new roles for DNA in generating three-dimensional lattices. These may be the result of a fascinating property of what is already a most fascinating biopolymer.

Experimental Section

Hybrid synthesis: Tetrakis(4-hydroxyphenyl)-methane[27] (TPM) was synthesized in two steps, starting from 4,4′,4′′-trimethoxytrityl chloride in 77% yield. The first strand of the DNA hybrid was constructed in a 5′→3′ direction, using 5′-phosphoramidites. After phosphitylation with 2-cyanoethyl-*N*,*N*-diisopropylchlorophosphoramidite, TPM was coupled for 30 min in a microwave-assisted coupling catalyzed by tetrazole (0.45 M in acetonitrile). Chain assembly of the remaining three DNA strands was achieved by automated synthesis with conventional 3′-phosphoramidites. Removal of the base-labile protecting groups and cleavage from the solid support were carried out with conc. aqueous ammonia at 55 °C for 5 h. Hybrids with dimer or non-self-complementary tetramer chains were purified by a two-stage cartridge purification on C18 phases. Hybrids with self-complementary tetramer or hexamer sequences were purified by preparative ion exchange HPLC. Samples were desalted by size-exclusion chromatography using Sephadex G-25. For detailed protocols and analytical data, please see the Supporting Information.

UV-melting analysis: UV-melting curves were acquired on a Perkin Elmer Lambda 750 spectrometer as heating and cooling curves with detection at 260 nm and gradients of 1 °C min $^{-1}$. The melting temperatures were determined from the extremum of the first derivative of 95-point smoothed curves.

Acknowledgements

This work was supported by CFN (sub-projects No.C5.1–3). The authors thank N. Griesang, A. Patra, and L. Reichenbach for sharing results, C. Deck for unmodified DNA, and H. Puchta for discussions.

Keywords: assembly · DNA · hybrids · nanostructures · oligonucleotides

[1] P. W. K. Rothemund, *Nature* **2006**, *440*, 297 302.
[2] Selected references: a) N. C. Seeman, *Acc. Chem. Res.* **1997**, *30*, 357 363; b) R. P. Goodman, I. A. T. Schaap, C. F. Tardin, C. M. Erben, R. M. Berry, C. F. Schmidt, A. J. Turberfield, *Science* **2005**, *310*, 1661 1665; c) J. Zimmermann, M. P. J. Cebulla, S. Mönninghoff, G. von Kiedrowski, *Angew. Chem.* **2008**, *120*, 3682 3686; *Angew. Chem. Int. Ed.* **2008**, *47*, 3626 3630.
[3] Selected recent reviews: a) N. C. Seeman, *Nature* **2003**, *421*, 427 431; b) K. V. Gothelf, T. H. LaBean, *Org. Biomol. Chem.* **2005**, *3*, 4023 4037; c) U. Feldkamp, C. M. Niemeyer, *Angew. Chem.* **2006**, *118*, 1888 1910; *Angew. Chem. Int. Ed.* **2006**, *45*, 1856 1876.
[4] D. Y. Zhang, A. J. Turberfield, B. Yurke, E. Winfree, *Science* **2007**, *318*, 1121 1125.
[5] a) C. A. Mirkin, R. L. Letsinger, R. C. Mucic, J. J. Storhoff, *Nature* **1996**, *382*, 607 609; b) A. P. Alivisatos, K. P. Johnsson, X. Peng, T. E. Wilson, C. J. Loweth, M. P. Jr Bruchez, P. G. Schultz, *Nature* **1996**, *382*, 609 611; c) P. Hazarika, B. Ceyhan, C. M. Niemeyer, *Angew. Chem.* **2004**, *116*, 6631 6633; *Angew. Chem. Int. Ed.* **2004**, *43*, 6469 6471.
[6] a) J. M. Nam, S. I. Stoeva, C. A. Mirkin, *J. Am. Chem. Soc.* **2004**, *126*, 5932 5933; b) N. L. Rosi, C. A. Mirkin, *Chem. Rev.* **2005**, *105*, 1547 1562.
[7] Selected references: a) C. M. Erben, R. P. Goodman, A. J. Turberfield, *Angew. Chem.* **2006**, *118*, 7574 7577; *Angew. Chem. Int. Ed.* **2006**, *45*, 7414 7417; b) G. Rasched, D. Ackermann, T. L. Schmidt, P. Broekmann, A. Heckel, M. Famulok, *Angew. Chem.* **2008**, *120*, 981 984; *Angew. Chem. Int. Ed.* **2008**, *47*, 967 970; c) R. Tel Vered, O. Yehezkeli, H. B. Yildiz, O. I. Wilner, I. Willner, *Angew. Chem.* **2008**, *120*, 8396 8400; *Angew. Chem. Int. Ed.* **2008**, *47*, 8272 8276.
[8] Selected references: a) N. C. Seeman, P. S. Lukeman, *Rep. Prog. Phys.* **2005**, *68*, 237 270; b) J. Malo, J. C. Mitchell, C. Venien Bryan, J. R. Harris, H. Wille, D. J. Sherratt, A. J. Turberfield, *Angew. Chem.* **2005**, *117*, 3117 3121; *Angew. Chem. Int. Ed.* **2005**, *44*, 3057 3061; c) Y. He, Y. Chen, H. P. Liu, A. E. Ribbe, C. D. Mao, *J. Am. Chem. Soc.* **2005**, *127*, 12202 12203; d) M. Slim, N. Durisic, P. Grutter, H. F. Sleiman, *ChemBioChem* **2007**, *8*, 804 812.
[9] P. J. Paukstelis, *J. Am. Chem. Soc.* **2006**, *128*, 6794 6795.
[10] W. Saenger, *Principles of Nucleic Acid Structure*, Springer, New York, **1984**.
[11] M. Mammen, S. K. Choi, G. M. Whitesides, *Angew. Chem.* **1998**, *110*, 2908 2953; *Angew. Chem. Int. Ed.* **1998**, *37*, 2754 2794.
[12] R. Jin, G. Wu, Z. Li, C. A. Mirkin, G. C. Schatz, *J. Am. Chem. Soc.* **2003**, *125*, 1643 1654.
[13] J. Xu, S. L. Craig, *J. Am. Chem. Soc.* **2005**, *127*, 13227 13231.
[14] P. L. Biancaniello, A. J. Kim, J. C. Crocker, *Phys. Rev. Lett.* **2005**, *94*, 058302/1 058302/4.
[15] J. M. Gibbs, S. J. Park, D. R. Anderson, K. J. Watson, C. A. Mirkin, S. T. Nguyen, *J. Am. Chem. Soc.* **2005**, *127*, 1170 1178.
[16] D. Nykypanchuk, M. M. Maye, D. van der Lelie, O. Gang, *Nature* **2008**, *451*, 549 552.
[17] S. Y. Park, A. K. R. Lytton Jean, B. Lee, S. Weigand, G. C. Schatz, C. A. Mirkin, *Nature* **2008**, *451*, 553 556.
[18] a) P. J. Paukstelis, J. Nowakowski, J. J. Birktoft, N. C. Seeman, *Chem. Biol.* **2004**, *11*, 1119 1126; b) M. Egli, *Chem. Biol.* **2004**, *11*, 1027 1029.
[19] B. R. Stepp, J. M. Gibbs Davis, D. L. F. Kohn, S. T. Nguyen, *J. Am. Chem. Soc.* **2008**, *130*, 9628 9629.
[20] M. Scheffler, A. Dorenbeck, S. Jordan, M. Wustefeld, G. von Kiedrowski, *Angew. Chem.* **1999**, *111*, 3513 3518; *Angew. Chem. Int. Ed.* **1999**, *38*, 3311 3315.
[21] L. H. Eckardt, K. Naumann, W. M. Pankau, M. Rein, M. Schweitzer, N. Windhab, G. von Kiedrowski, *Nature* **2002**, *420*, 286.
[22] a) K. M. Stewart, J. Rojo, L. W. McLaughlin, *Chem. Commun.* **2003**, 2934 2935; b) K. M. Stewart, L. W. McLaughlin, *J. Am. Chem. Soc.* **2004**, *126*, 2050 2057; c) K. M. Stewart, J. Rojo, L. W. McLaughlin, *Angew. Chem.* **2004**, *116*, 5932 5935; *Angew. Chem. Int. Ed.* **2004**, *43*, 5808 5811.
[23] M. S. Shchepinov, K. U. Mir, J. K. Elder, M. D. Frank Kamenetskii, E. M. Southern, *Nucleic Acids Res.* **1999**, *27*, 3035 3041.
[24] F. A. Aldaye, H. F. Sleiman, *Angew. Chem.* **2006**, *118*, 2262 2267; *Angew. Chem. Int. Ed.* **2006**, *45*, 2204 2209.
[25] E. V. Shevchenko, D. V. Talapin, N. A. Kotov, S. O'Brien, C. B. Murray, *Nature* **2006**, *439*, 55 59.
[26] S. J. Hurst, H. D. Hill, C. A. Mirkin, *J. Am. Chem. Soc.* **2008**, *130*, 12192 12200.
[27] J. H. Fournier, X. Wang, J. D. Wuest, *Can. J. Chem.* **2003**, *81*, 376 380.